METHODOLOGIES FOR THE NUMERICAL SIMULATION OF FLUID FLOW IN INTERNAL COMBUSTION ENGINES

Ezequiel J. López

Director: Norberto M. Nigro
Codirector: Mario A. Storti

Centro Internacional de Métodos Computacionales en Ingeniería
Universidad Nacional del Litoral
Santa Fe, Argentina
web page: http://www.cimec.org.ar/
e-mail: ejlopez@santafe-conicet.gov.ar

Problem statement

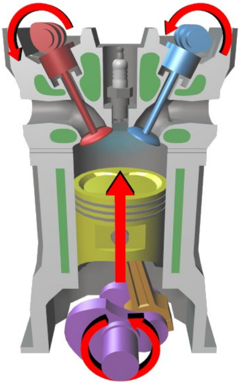

Problem statement

Main characteristics of in-cylinder flow problems in internal combustion (IC) engines

- Turbulent viscous compressible flow.

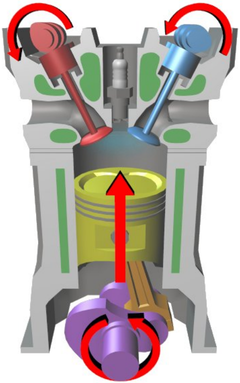

Problem statement

Main characteristics of in-cylinder flow problems in internal combustion (IC) engines

- Turbulent viscous compressible flow.
- 3D moving domains with complex geometry, high deformation and topological changes.

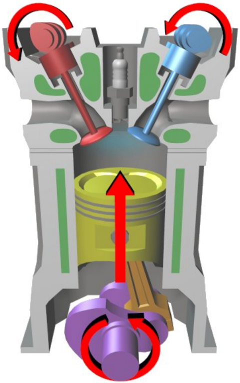

Problem statement

Main characteristics of in-cylinder flow problems in internal combustion (IC) engines

- Turbulent viscous compressible flow.
- 3D moving domains with complex geometry, high deformation and topological changes.
- Low Mach number flow during the major fraction of the cycle.

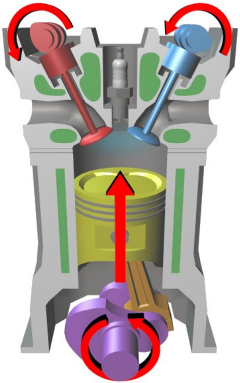

Problem statement

Main characteristics of in-cylinder flow problems in internal combustion (IC) engines

- Turbulent viscous compressible flow.
- 3D moving domains with complex geometry, high deformation and topological changes.
- Low Mach number flow during the major fraction of the cycle.
- Reactive flow.

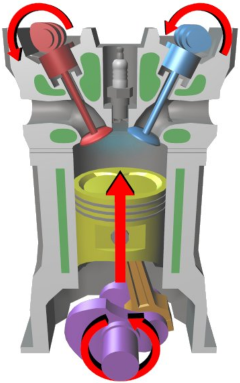

Problem statement

Main characteristics of in-cylinder flow problems in internal combustion (IC) engines

- Turbulent viscous compressible flow.
- 3D moving domains with complex geometry, high deformation and topological changes.
- Low Mach number flow during the major fraction of the cycle.
- Reactive flow.
- Fuel injection (spray dynamics).

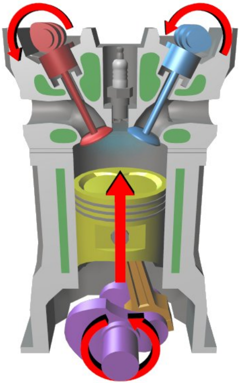

Problem statement

Main characteristics of in-cylinder flow problems in internal combustion (IC) engines

- Turbulent viscous compressible flow.
- 3D moving domains with complex geometry, high deformation and topological changes.
- Low Mach number flow during the major fraction of the cycle.
- Reactive flow.
- Fuel injection (spray dynamics).
- Dynamic boundary conditions.

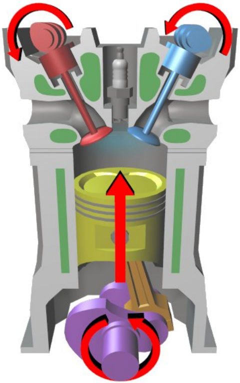

Problem statement

Main characteristics of in-cylinder flow problems in internal combustion (IC) engines

- Turbulent viscous compressible flow.
- 3D moving domains with complex geometry, high deformation and topological changes.
- Low Mach number flow during the major fraction of the cycle.
- Reactive flow.
- Fuel injection (spray dynamics).
- Dynamic boundary conditions.

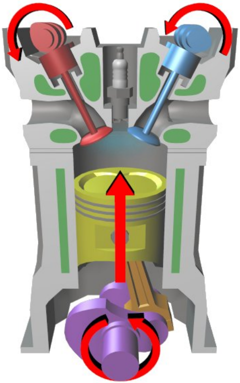

Navier-Stokes equations

Using an ALE (Arbitrary Lagrangian Eulerian) strategy, the system of Navier-Stokes equations in its quasi-linear form can be written as

$$\frac{\partial \mathbf{U}}{\partial t} + (\mathbf{A}_i - w_i \mathbf{I}) \frac{\partial \mathbf{U}}{\partial x_i} = \frac{\partial}{\partial x_i} \left(\mathbf{K}_{ij} \frac{\partial \mathbf{U}}{\partial x_j} \right) + \mathbf{S} \quad \text{on } \Omega_t \times (0, t_\mathrm{f})$$

Boundary conditions at solid walls

- Condition on the flow velocity.
- Condition on the temperature or the heat flux.

Boundary conditions at inlet/outlet

- Dynamic absorbing boundary conditions.

Numerical implementation

- The equations are discretized in space using the Finite Element Method (FEM).
- The method is stabilized by means of the Streamline-Upwind/Petrov-Galerkin (SUPG) technique.
- An isotropic shock-capturing strategy is included in order to stabilize the computations in the presence of sharp gradients.
- The trapezoidal difference scheme is applied for time discretization.
- The absorbing boundary conditions are applied using Lagrange multipliers.

Numerical implementation

'Mixed' absorbing/wall boundary conditions

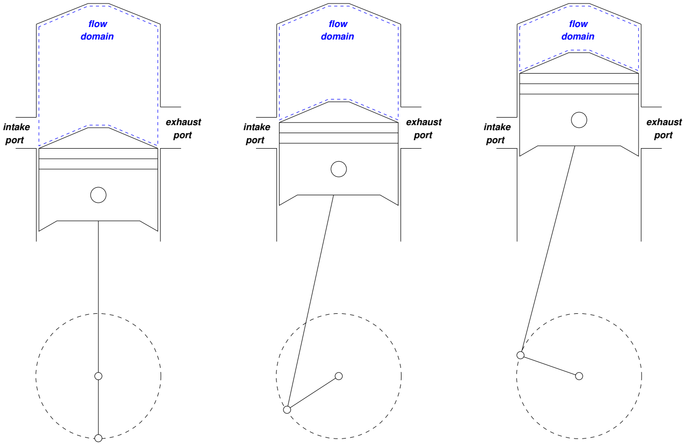

Numerical implementation

‘Mixed’ absorbing/wall boundary conditions (cont.)

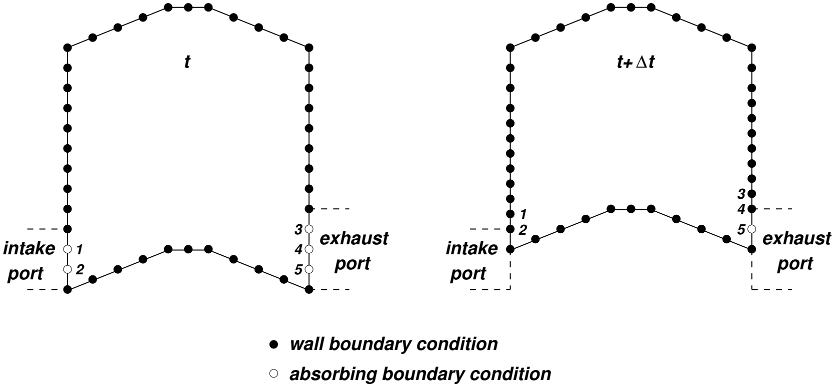

Mesh dynamics

Motivation

Mesh dynamics

Motivation

Remeshing

- A body-conforming mesh has to be regenerated at each time step.
- The projection of solutions from a mesh to another one is needed.
- When implicit schemes are applied in an environment of parallel computing, the matrix profile must be calculated at each remeshing stage.

Mesh dynamics

Motivation

Remeshing

- A body-conforming mesh has to be regenerated at each time step.
- The projection of solutions from a mesh to another one is needed.
- When implicit schemes are applied in an environment of parallel computing, the matrix profile must be calculated at each remeshing stage.

Mesh movement

- The motion of the grid could cause the deterioration of the mesh quality and, in some situations, generate an invalid mesh.

The mesh dynamics strategy

Functional design

The CMD (Computational Mesh Dynamics) strategy developed could be classified as a mesh smoothing method and it is based on an optimization problem, where the functional (F) is defined in terms of some appropriate element quality indicator.

The mesh dynamics strategy

Functional design

The CMD (Computational Mesh Dynamics) strategy developed could be classified as a mesh smoothing method and it is based on an optimization problem, where the functional (F) is defined in terms of some appropriate element quality indicator.

Some design conditions for F are:

- F should be computed from element contributions.
- The minimum of F should give the best mesh quality.
- F should be well behaved enough in order to solve the minimization problem with Newton-like methods.
- F should be convex in order to guarantee uniqueness of the minimum and positivity of the stiffness matrices.

Functional design

Expression for the element functional proposed

$$F_e = C_{\mathrm{v}} \left(\frac{V_e}{V_{\mathrm{ref}}^e} - 1 \right)^m + C_{\mathrm{q}} q_e^n, \quad m \text{ even}, \; n < 0$$

Functional design

Expression for the element functional proposed

$$F_e = C_{\mathrm{v}} \left(\frac{V_e}{V^e_{\mathrm{ref}}} - 1 \right)^m + C_{\mathrm{q}} q_e^n, \quad m \text{ even}, \; n < 0$$

Element quality indicator applied

$$q = C \left[\sum_{i=1}^{N} \left(q_{S,i} \right)^n \right]^{1/n}$$

where

$$q_S = \frac{V}{S_e}, \quad S_e = \sum_j l_j^{n_{\mathrm{d}}}$$

Results

Step 2D

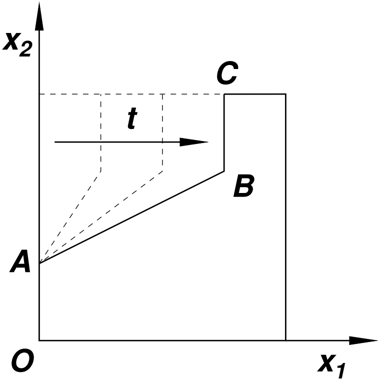

- Imposed displacements on boundary nodes.

Results

Step 2D

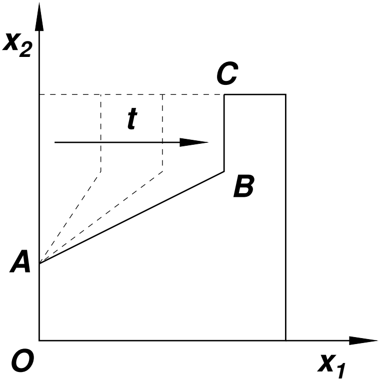

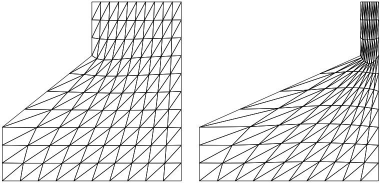

50 % def. 90 % def.

- Imposed displacements on boundary nodes.

Results

Step 2D

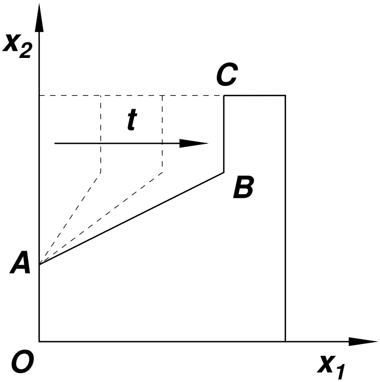

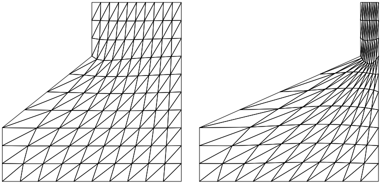

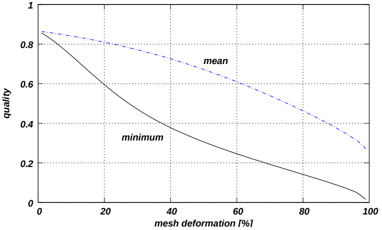

- Imposed displacements on boundary nodes.

Results

Step 3D

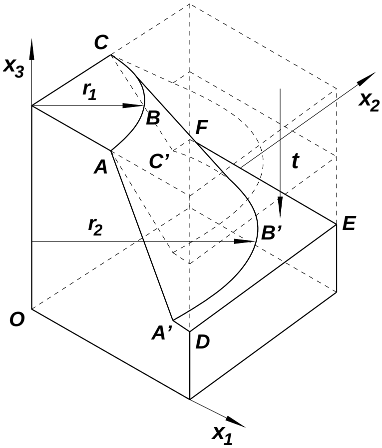

Results

Step 3D

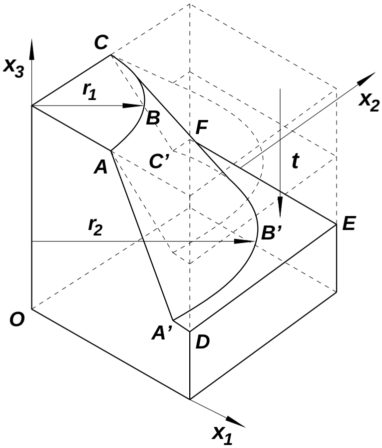

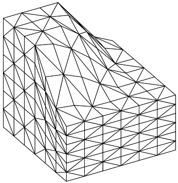

50 % def.

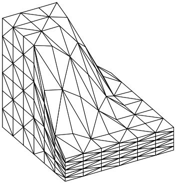

80 % def.

Results

Step 3D

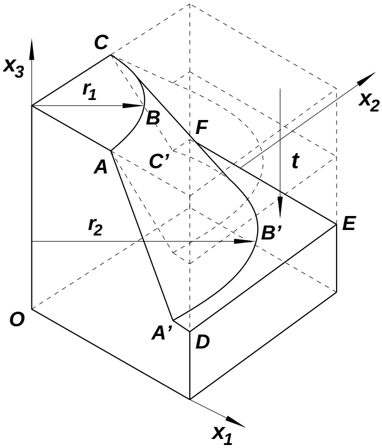

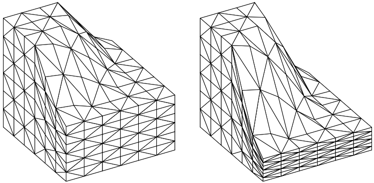

50 % def.

80 % def.

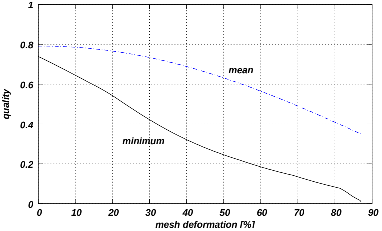

Functional regularization

- $F \to \infty$ when $q_e \to 0$ (for simplicial elements, $V_e \to 0$).

Functional regularization

- $F \to \infty$ when $q_e \to 0$ (for simplicial elements, $V_e \to 0$).

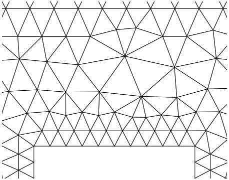

$t = 0$

Functional regularization

- $F \to \infty$ when $q_e \to 0$ (for simplicial elements, $V_e \to 0$).

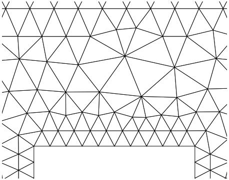

$t = 0$

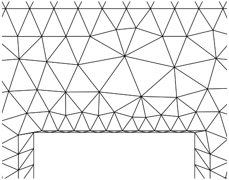

$t = \Delta t_{\mathrm{CMD}}$

(Valid mesh)

Functional regularization

- $F \rightarrow \infty$ when $q_e \rightarrow 0$ (for simplicial elements, $V_e \rightarrow 0$).

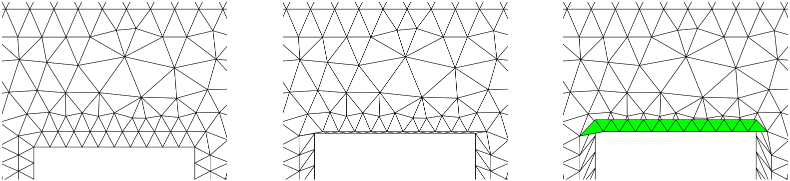

$t = 0$

$t = \Delta t_{\mathrm{CMD}}$ (Valid mesh)

$t = \Delta t_{\mathrm{CFD}}$ (Tangled mesh)

Functional regularization

- $F \to \infty$ when $q_e \to 0$ (for simplicial elements, $V_e \to 0$).

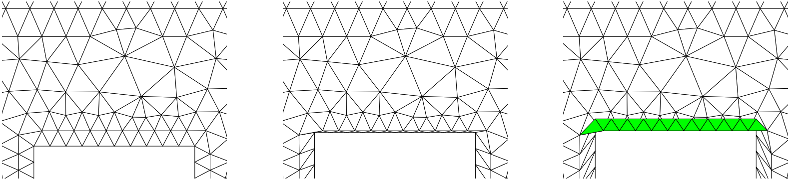

$t = 0$ $t = \Delta t_{\mathrm{CMD}}$ (Valid mesh) $t = \Delta t_{\mathrm{CFD}}$ (Tangled mesh)

- The CMD strategy presented requires valid meshes at the begin of each time step and, thus, conditioning the Δt.

Functional regularization

- The functional is regularized by replacing the volume in the expression of the element quality indicator by the function

$$h(V) = \frac{1}{2}\left(V + \sqrt{V^2 + 4\delta^2}\right)$$

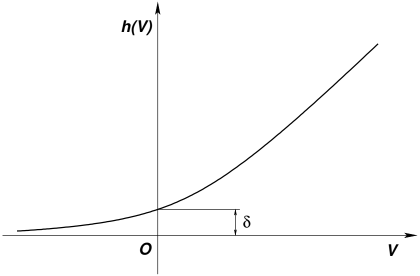

- For $V > 0$, $h(V) \rightarrow V$ when $\delta \rightarrow 0$.

Simultaneous mesh untangling and smoothing

- $\delta > 0$ is needed in the untangling stage.
- $\delta \rightarrow 0$ is needed in the smoothing stage.
- Defining a decreasing sequence $\{\delta^k\}$ such that $\delta^k \rightarrow 0$ when $k \rightarrow \infty$, a simultaneous mesh untangling and smoothing technique is obtained.

Simultaneous mesh untangling and smoothing

- $\delta > 0$ is needed in the untangling stage.
- $\delta \to 0$ is needed in the smoothing stage.
- Defining a decreasing sequence $\{\delta^k\}$ such that $\delta^k \to 0$ when $k \to \infty$, a simultaneous mesh untangling and smoothing technique is obtained.

For the tests, the following convergence criteria is applied:

- Valid mesh.
- For the iteration k, $\dfrac{|q^k_{\mathrm{mesh}} - q^{k-1}_{\mathrm{mesh}}|}{q^k_{\mathrm{mesh}}} < \epsilon_{\mathrm{q}}$, being $q_{\mathrm{mesh}} = \min_e q_e$ and $\epsilon_{\mathrm{q}} > 0$ a prefixed tolerance.

Results

Step 2D

- Imposed displacement on boundary nodes.
- Solved in 1 time step.

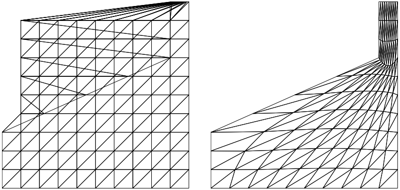

Results

Step 2D

- Imposed displacement on boundary nodes.
- Solved in 1 time step.

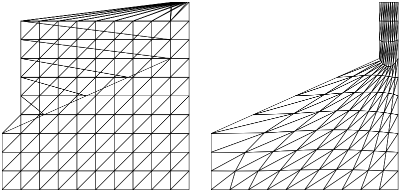

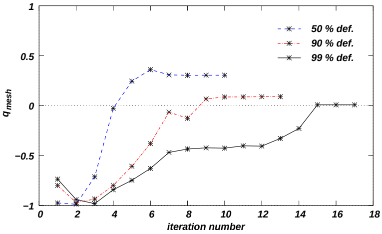

Results

Step 2D

- Imposed displacement on boundary nodes.
- Solved in 1 time step.

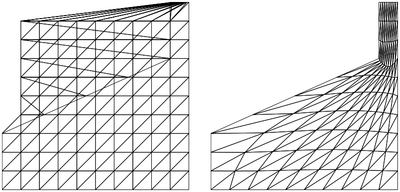

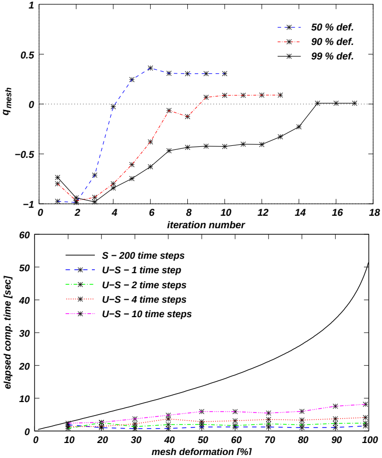

Results

Step 3D

- Imposed displacement on boundary nodes.
- Solved in 1 time step.

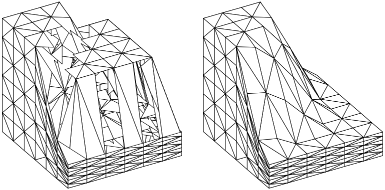

Results

Step 3D

- Imposed displacement on boundary nodes.
- Solved in 1 time step.

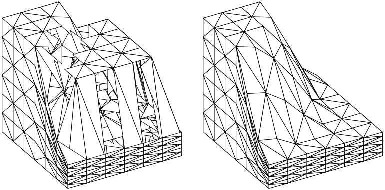

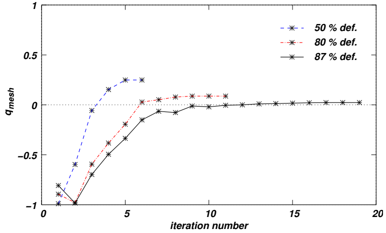

Results

Step 3D

- Imposed displacement on boundary nodes.
- Solved in 1 time step.

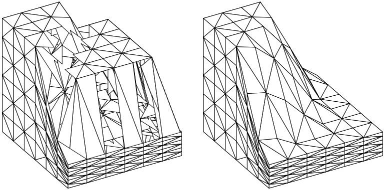

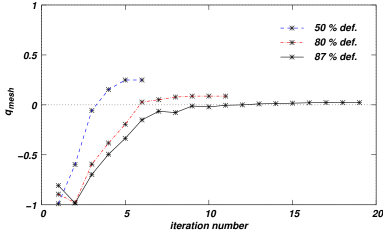

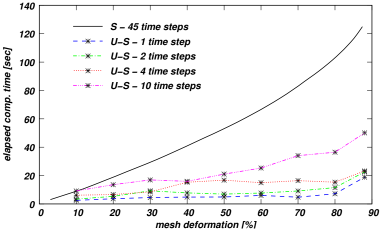

Results

Axisymmetrical flowmeter

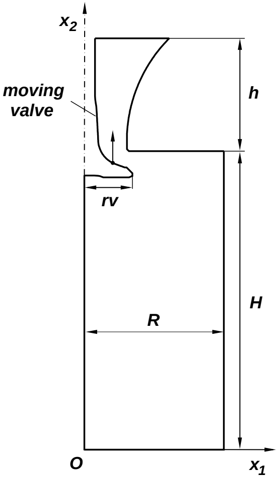

- Nodes on the cylinder walls and on the valve stem are free to slide.
- The remaining nodes have their displacement imposed.

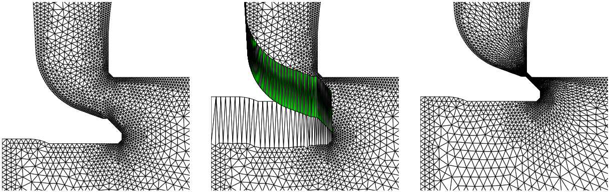

Results

Diesel engine with three valves

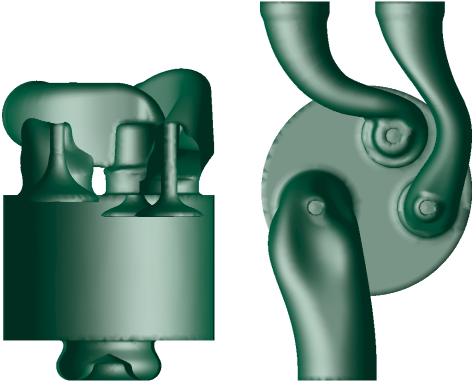

- Sliding nodes on cylinder walls and valve stems.
- Imposed displacements on remaining nodes.
- $\Delta\theta = 1^\circ$.
- Initial $q_{\mathrm{mesh}} = 0.0211$.

Results

Diesel engine with three valves

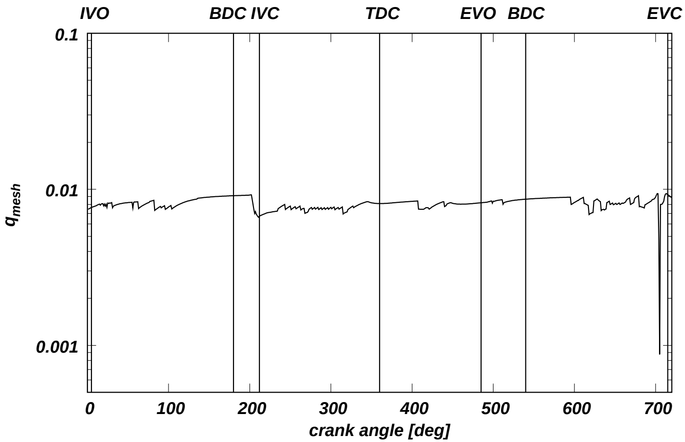

Results

Diesel engine with three valves

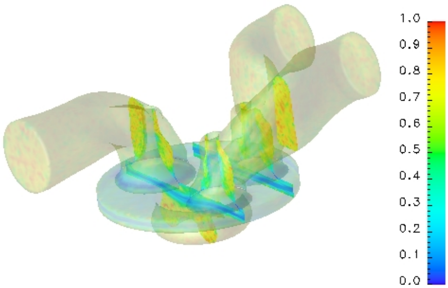

Resolution of compressible flows with low Mach numbers

Motivation

Resolution of compressible flows with low Mach numbers

Motivation

Strategies proposed in the bibliography to solve flows in the low Mach number limit:

- The modification of compressible solvers (density based), *e. g.*, preconditioning and asymptotic methods.
- The extension of incompressible solvers (pressure based), *e. g.*, artificial compressibility.
- Unified formulations compressible-incompressible.

Resolution of compressible flows with low Mach numbers

Motivation

Strategies proposed in the bibliography to solve flows in the low Mach number limit:

- The modification of compressible solvers (density based), *e. g.*, preconditioning and asymptotic methods.
- The extension of incompressible solvers (pressure based), *e. g.*, artificial compressibility.
- Unified formulations compressible-incompressible.

It is proposed to use the method of preconditioning due to its ability to work in a wide range of Mach and Reynolds numbers.

Problem definition

- The preconditioning method in conjunction with the ‘dual-time-stepping’ technique are applied.
- If $\boldsymbol{\Gamma}$ denotes the preconditioning matrix, the modified system of equations is written as

$$\boldsymbol{\Gamma}\frac{\partial \mathbf{U}}{\partial \tau} + \frac{\partial \mathbf{U}}{\partial t} + (\mathbf{A}_i - w_i\mathbf{I})\frac{\partial \mathbf{U}}{\partial x_i} = \frac{\partial}{\partial x_i}\left(\mathbf{K}_{ij}\frac{\partial \mathbf{U}}{\partial x_j}\right) + \mathbf{S}$$

- Physical time: t; pseudo-time: τ.

Two CFL (Courant-Friedrichs-Levy) numbers are considered

$$CFL_c = \frac{c\Delta t}{h} \quad \text{and} \quad CFL_u = \frac{\|\mathbf{u}\|\Delta t}{h}$$

Problem definition

The preconditioning matrix used was proposed by Choi and Merkle to solve steady compressible flows with the Finite Volume Method. The ‘free’ parameters involved in $\mathbf{\Gamma}$ are the following:

- M_{r}: reference Mach number. It replaces the Mach number and was originally introduced to avoid the singularities that appears when $M \rightarrow 0$.
- β: parameter adjustment for viscous regions.
- δ: coefficient of the time derivative of pressure in the energy equation.

Preconditioning strategies

The definition of M_{r} allows to choose among different preconditioning matrices:

- 'Steady preconditioning' (SP), proposed by Choi and Merkle
$$M_{\mathrm{r}} = \min(1, \max(M, M_{\epsilon}))$$
- 'Unsteady preconditioning' (UP), proposed by Vigneron *et al.*
$$M_{\mathrm{r}} = \min(1, \max(\sqrt{M^2 + CFL_c^{-2}}, M_{\epsilon}))$$
- Non-preconditioned (NP), for $\delta = 1$

$$M_{\mathrm{r}} = [\gamma - (\gamma - 1)\delta]^{-1/2}$$

Condition number of the system

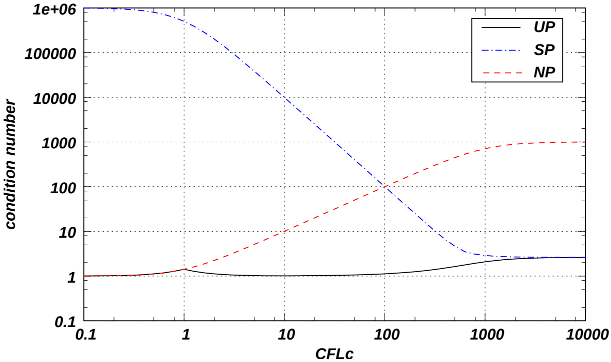

Condition number as a function of CFL_c with $M = 1 \times 10^{-3}$ and $M_\epsilon = 1 \times 10^{-6}$ for the inviscid case.

Condition number of the system

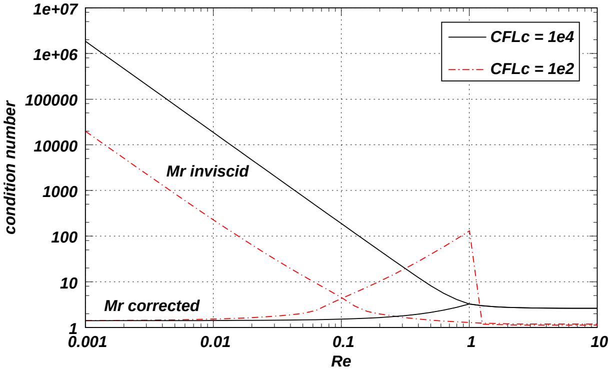

Condition number as a function of CFL_c for several Reynolds numbers with the reference Mach for the inviscid case ($M = 1 \times 10^{-3}$).

Condition number of the system

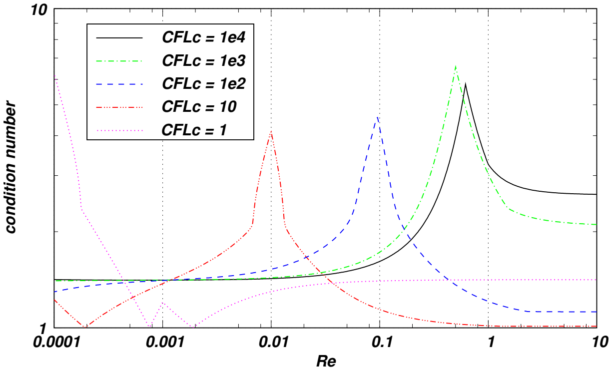

Condition number as a function of the Reynolds number for several CFL_c numbers for the viscous case. $M = 1 \times 10^{-3}$ and $M_\epsilon = 1 \times 10^{-6}$.

Numerical implementation

- The equations are discretized in space using FEM.
- The SUPG strategy is applied to stabilize the scheme.
- The matrix of intrinsic time scale is computed with the maximum eigenvalue of the advective jacobian.
- An implicit formulation is applied in time and pseudo-time.
- The derivative with respect to the pseudo-time is discretized using the backward Euler difference scheme.

Results

Flow in a channel with a moving indentation

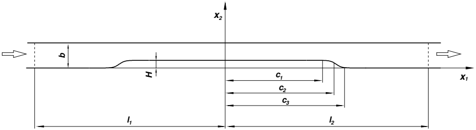

- $M = U/c = 2.67 \times 10^{-3}$, $Re = \rho U b/\mu = 507$.
- Velocity and density imposed on inlet section.
- Isothermal walls.
- No-slip boundary condition on the walls.
- Dynamic absorbing boundary condition on outlet section.

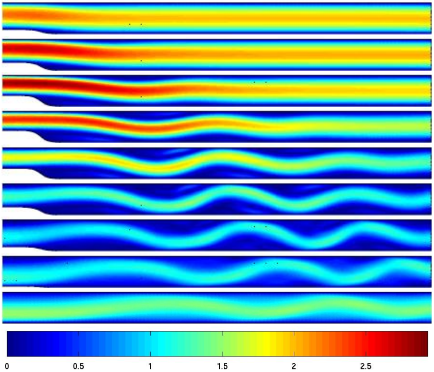

Magnitude of flow velocity [m/s] - NSI

Results

Flow in a channel with a moving indentation

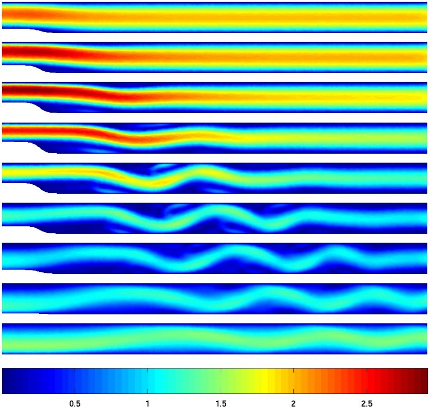

Magnitude of flow velocity [m/s] - UP

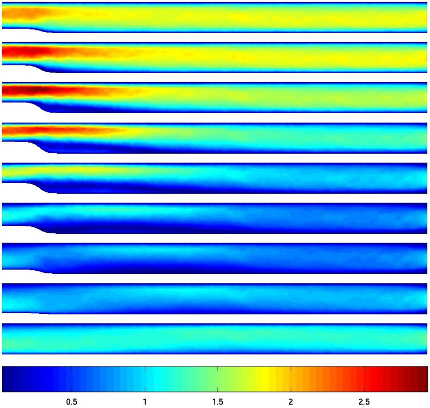

Magnitude of flow velocity [m/s] - NP

Results

Flow in a channel with a moving indentation

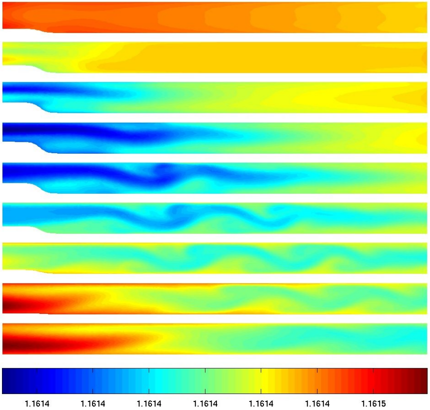

Density [kg/m^3] - UP

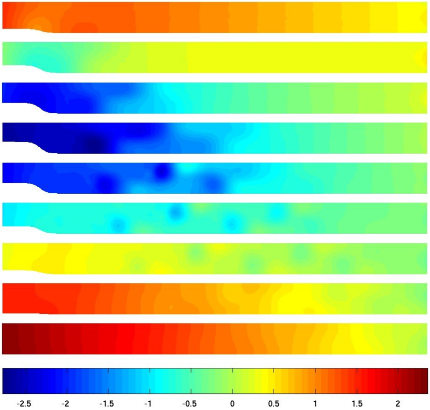

Pressure perturbation [Pa] - UP

Results

Flow in a channel with a moving indentation

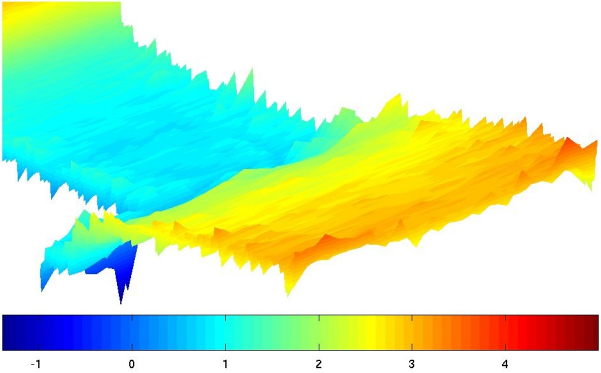

Pressure perturbation field ([Pa]) at $t^* = 0.5$ - NP.

Results

Flow in a channel with a moving indentation

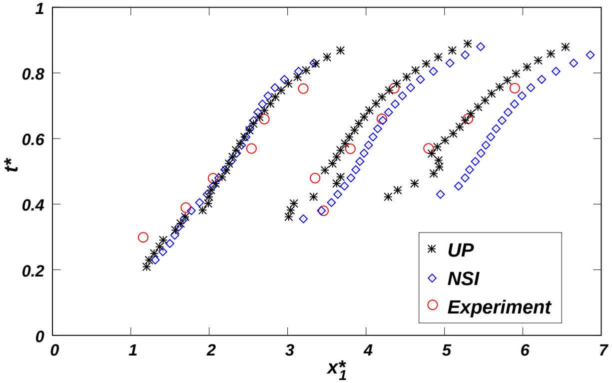

Comparison of predicted and experimentally observed positions of the first three vortexes center.

Results

In-cylinder flow in an opposed-piston engine

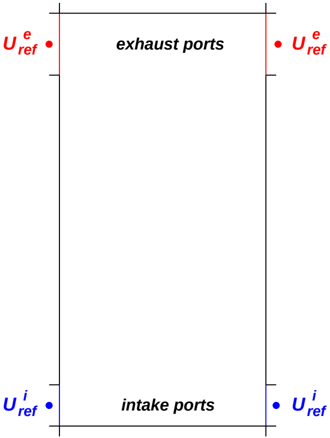

Results

In-cylinder flow in an opposed-piston engine

- $N = 3000$ rpm.
- Without combustion.
- No-slip boundary condition on solid walls.
- Insulated solid walls.
- Dynamic boundary conditions on intake/exhaust ports (mixed absorbing/wall).
- $CFL_u\, \mathcal{O}(1)$ along the whole simulation.

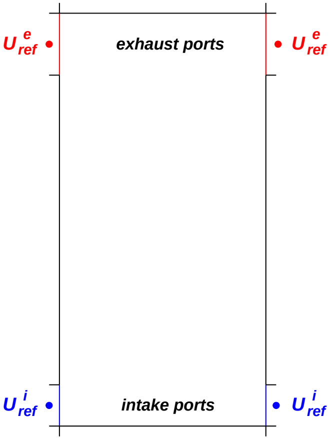

Results

In-cylinder flow in an opposed-piston engine

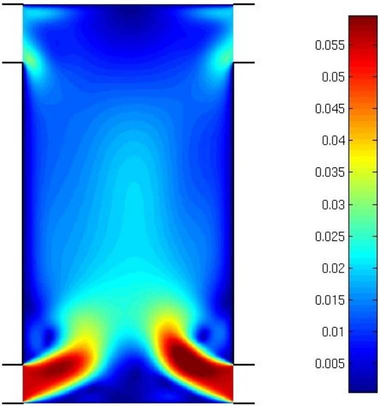

Coupling of 1D/multi-D domains for compressible flows

Motivation

Coupling of 1D/multi-D domains for compressible flows

Motivation

- Due to the computational cost, CFD-3D models are applied to simulate only a few components of an IC engine at each time.
- Usually, the boundary conditions for these 3D models are imposed by using 0D/1D codes.
- When dimensionally heterogeneous models are used, the need to perform the coupling between sub-domains arises.
- 1D/multi-D coupling will be considered.

Problem definition

1D/1D coupling

Let an 1D problem discretized by a grid with N elements

$$P \begin{cases} \mathbf{E}_1(\mathbf{U}_1, \mathbf{U}_2) = \mathbf{0} \\ \mathbf{E}_2(\mathbf{U}_1, \mathbf{U}_2, \mathbf{U}_3) = \mathbf{0} \\ \vdots \\ \mathbf{E}_{N+1}(\mathbf{U}_N, \mathbf{U}_{N+1}) = \mathbf{0} \end{cases}$$

Assumptions:

- The equation at node i involves only the nodal states at nodes $i-1$, i and $i+1$.
- The equation at node i can be separated in its right and left contributions

$$\mathbf{E}_i(\mathbf{U}_{i-1}, \mathbf{U}_i, \mathbf{U}_{i+1}) = \mathbf{E}_{i1}(\mathbf{U}_{i-1}, \mathbf{U}_i) + \mathbf{E}_{i2}(\mathbf{U}_i, \mathbf{U}_{i+1}) = \mathbf{0}$$

Problem definition

1D/1D coupling

The problem P is splitted into two sub-problems (P_1 y P_2)

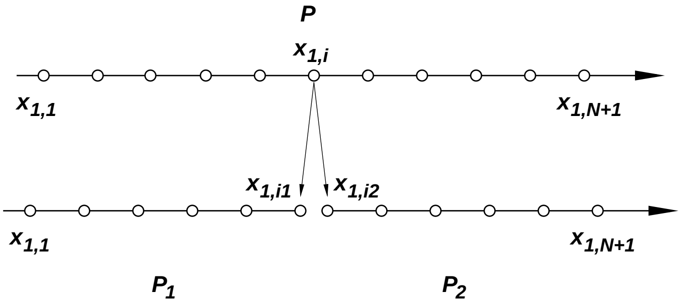

Coupling for implicit schemes 'monolithically' solved

1D/1D coupling

$$
\begin{cases}
\mathbf{E}_1(\mathbf{U}_1, \mathbf{U}_2) = \mathbf{0} \\
\mathbf{E}_2(\mathbf{U}_1, \mathbf{U}_2, \mathbf{U}_3) = \mathbf{0} \\
\vdots \\
\mathbf{E}_{i1}(\mathbf{U}_{i-1}, \mathbf{U}_{i1}) + \mathbf{U}_{\mathrm{lm}} = \mathbf{0} \\
\mathbf{U}_{i1} - \mathbf{U}_{i2} = \mathbf{0} \\
\mathbf{E}_{i2}(\mathbf{U}_{i2}, \mathbf{U}_{i+1}) - \mathbf{U}_{\mathrm{lm}} = \mathbf{0} \\
\vdots \\
\mathbf{E}_{N+1}(\mathbf{U}_N, \mathbf{U}_{N+1}) = \mathbf{0}
\end{cases}
$$

- The constraint $\mathbf{U}_{i1} = \mathbf{U}_{i2}$ imposes the continuity of the solution and forces the continuity of fluxes through the coupling interface.
- Useful when the contributions to the global residue and the global jacobian matrix from sub-domains are available.

Coupling for implicit schemes ‘monolithically’ solved

1D/multi-D coupling

In this case, the conditions at the coupling interface for the multi-D domain are defective.

- One possibility is to impose the constraints

$$\mathbf{U}_{1D} = \mathbf{U}^{i}_{MD} \quad i = 1, \ldots, M$$

- Another option is to impose the constraints

$$\int_S \mathbf{U}_{MD} dS = \int_S \mathbf{U}_{1D} dS = \mathbf{U}_{1D} S$$

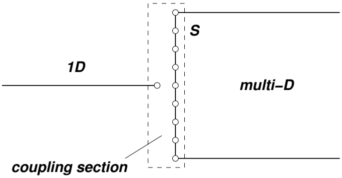

Results

1D/2D coupling: gas discharge from a reservoir

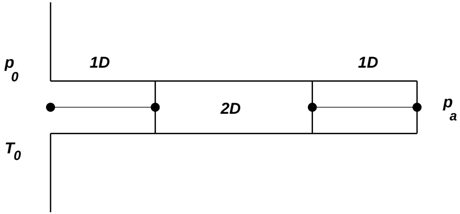

- $p_0 = 1.2 \times 10^5$ Pa
- $T_0 = 278.75$ K
- $p_a = 1 \times 10^5$ Pa
- $L = 7$ m

- Inviscid flow.
- Insulated walls and without friction.
- Density, pressure and normal velocity are equalized at coupling sections.

Results

1D/2D coupling: gas discharge from a reservoir

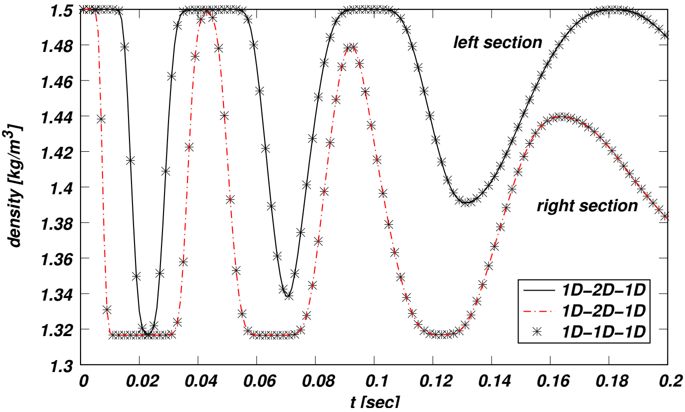

Results

1D/2D coupling: gas discharge from a reservoir

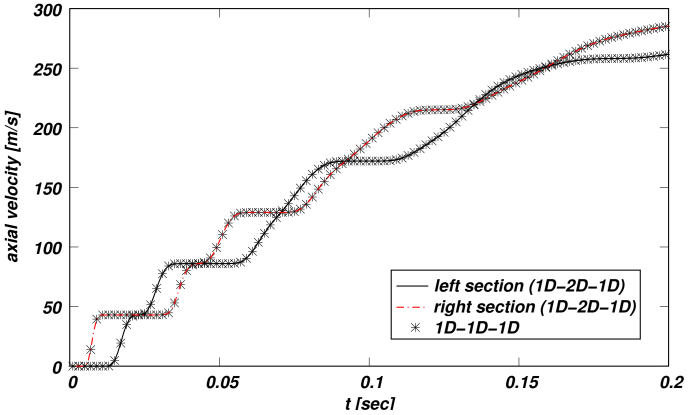

Results

1D/2D coupling: gas discharge from a reservoir

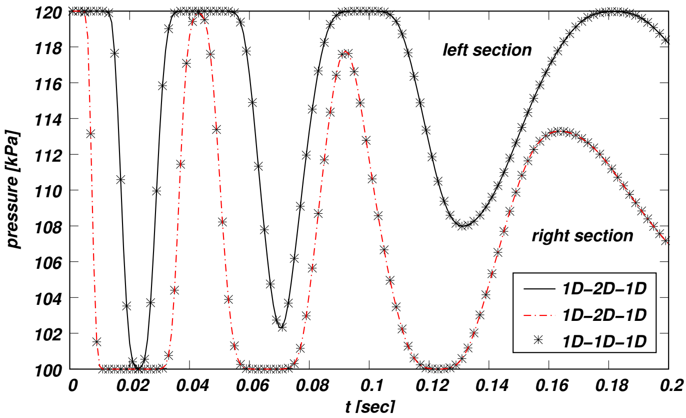

Results

1D/3D coupling: exhaust manifold branch

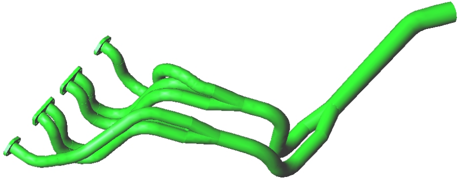

Results

1D/3D coupling: exhaust manifold branch

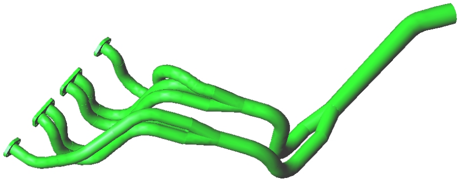

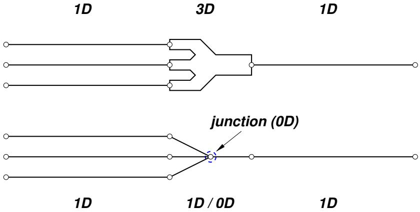

Results

1D/3D coupling: exhaust manifold branch

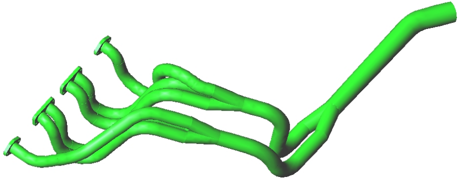

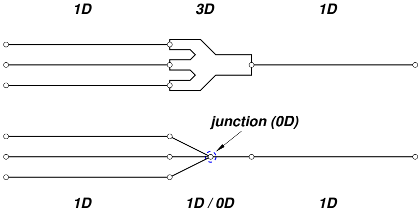

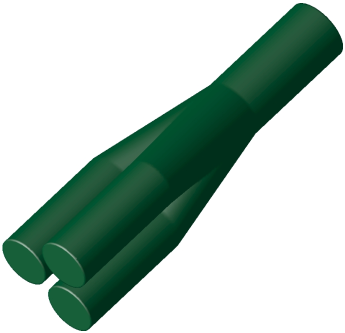

Results

1D/3D coupling: exhaust manifold branch

- $N = 8000$ rpm.
- Boundary conditions for the 3D model:
  - Slip boundary condition on solid walls.
  - Insulated walls.
- Boundary condition at the end of the 1D domains obtained from a 1D/0D simulation of the engine.
- Density, pressure and normal velocity are equalized at coupling sections.
- Tangential components of velocity at coupling sections are constrained to be zero.

Results

1D/3D coupling: exhaust manifold branch

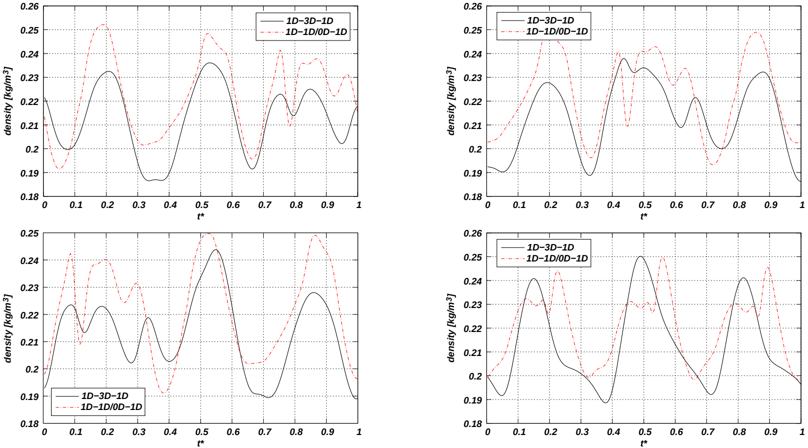

Results

1D/3D coupling: exhaust manifold branch

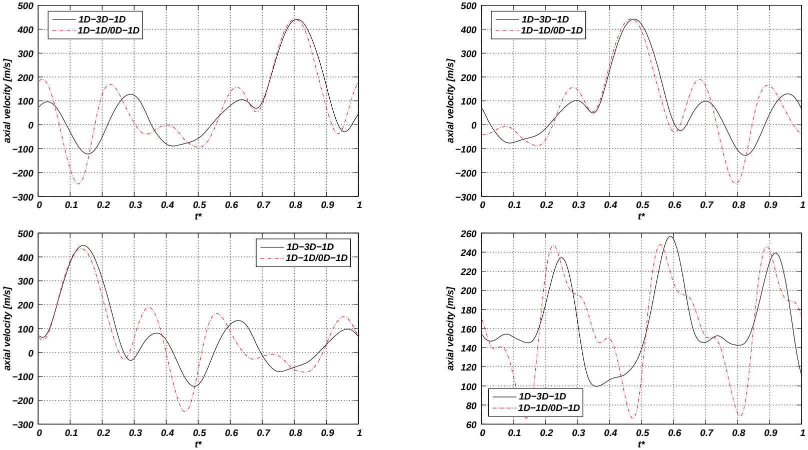

Results

1D/3D coupling: exhaust manifold branch

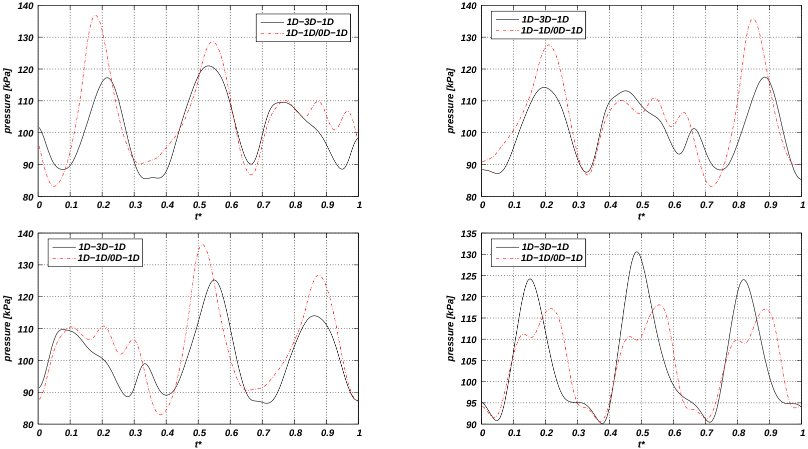

Numerical simulation of the fluid flow in the MRCVC

Description of the geometry

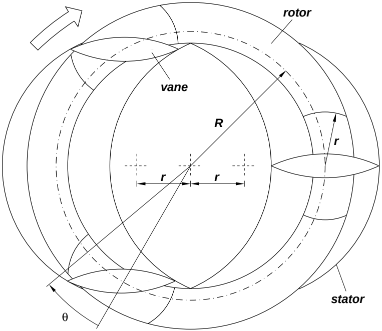

Numerical simulation of the fluid flow in the MRCVC

Description of the geometry

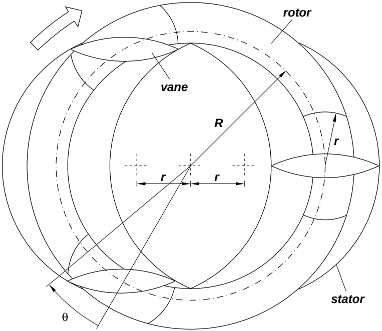

Main features of the engine:

- The combustion could be performed at constant volume.
- Cycle duration for a MRCVC with *n* vanes:

$$\Delta\theta = 2\pi\left(1 + \frac{2}{n}\right)$$

- There are $n+2$ operating chambers along a cycle.

Operation and geometry of the MRCVC

Changes in the flow domain

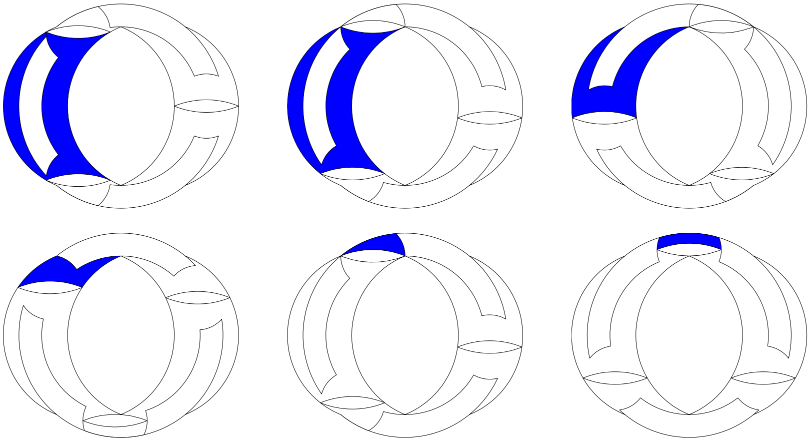

Numerical simulation of fluid flow in the MRCVC engine

- The fluid flow problem is solved using a 2D approximation.
- The engine simulated has $n = 3$ vanes.
- Maximum chamber volume: 500 cm^3.
- Geometric compression ratio: 9:1.
- Flow under cold conditions (without combustion).

The Computational Mesh Dynamics problem

- The proposed U-S strategy is applied.
- Imposed nodal boundary displacements.
- Triangular elements with $h = 0.2$ mm on the boundaries and $h = 0.5$ mm in the interior region of the domain.
- The mesh could be generated for a ‘stroke’ $\left(0 \leq \theta \leq \frac{n+2}{2n}\pi\right)$ and, then, to flip it around vertical and horizontal symmetry axis.

The Computational Mesh Dynamics problem

Quality of the mesh generated

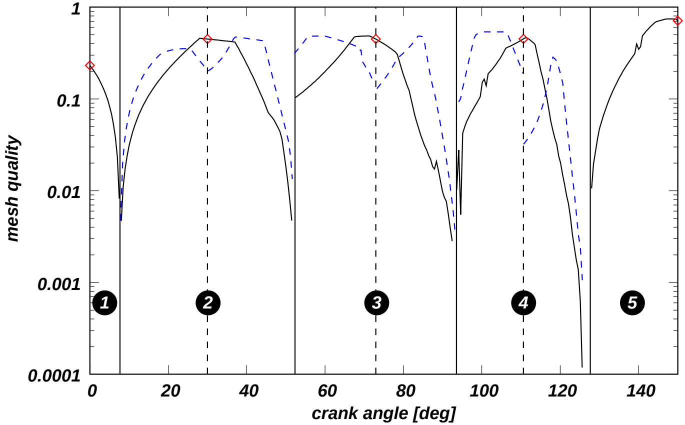

The Computational Mesh Dynamics problem

Quality of the mesh generated

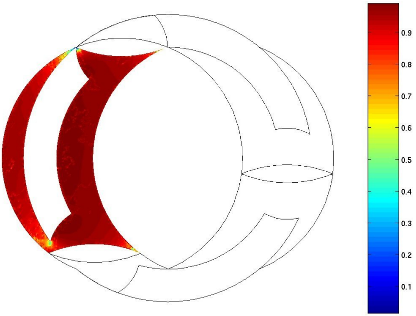

End sub-interval 1.

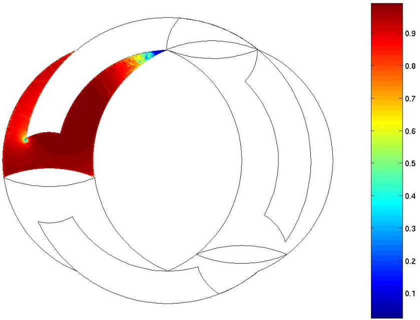

End sub-interval 2.

The Computational Mesh Dynamics problem

Quality of the mesh generated

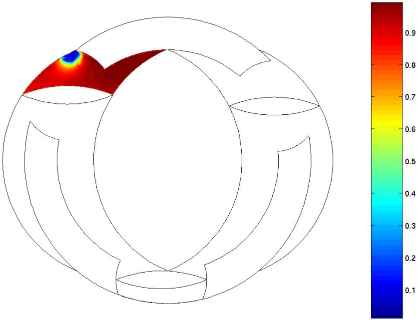

End sub-interval 3.

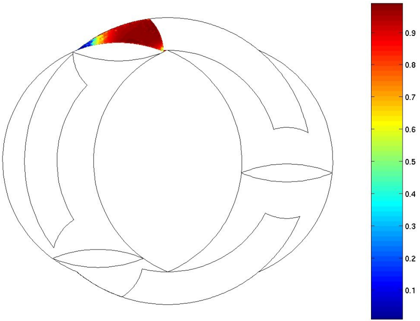

End sub-interval 4.

The Computational Fluid Dynamics problem

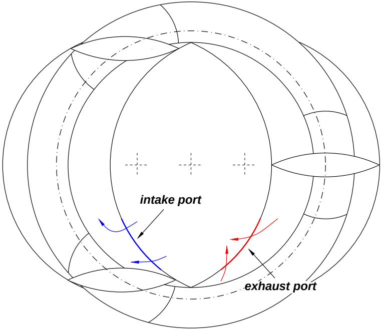

- No-slip boundary condition on solid walls.
- Insulated solid walls.
- Intake and exhaust ports modeled with ‘mixed’ absorbing/wall boundary conditions.
- $N = 3000$ rpm.

The Computational Fluid Dynamics problem

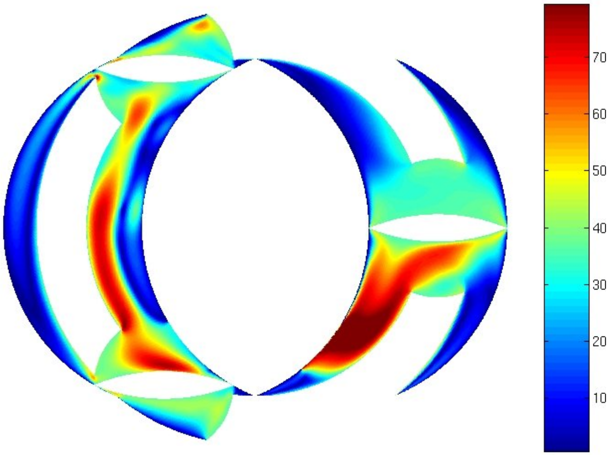

Conclusions

- The main goal of this thesis was the proposition, description and testing of some computational tools to solve in-chamber flows in IC engines.
- An optimization-based simultaneous mesh untangling and smoothing strategy was proposed to solve CMD problems.
  - The technique was successfully applied to solve the mesh movement in IC engines problems.
  - Under certain conditions, this strategy allows to generate conformal meshes in 2D.
- The preconditioning of the governing equations with the dual time stepping method were applied to solve transient compressible flows in the low-Mach number limit.

Conclusions

- A simple technique to solve the coupling of 1D/multi-D domains was applied in dimensionally heterogeneous computational models.
- A 0D/1D code able to describe IC engine operating characteristics was implemented and validated. This code is useful as a boundary condition generator for the multi-D simulations.
- The proposed techniques were incorporated into the CFD code that is developed at CIMEC (`PETSc-FEM`).
- The first steps towards the simulation of the fluid flow in the MRCVC engine chambers were done.

Conclusions

During this thesis it has been published/submitted the following articles:

- *A minimal element distortion strategy for computational mesh dynamics*; López, E.; Nigro, N.; Storti, M. and Toth, J.; Int. J. for Numerical Methods in Engineering 2007, Volume 69, Issue 9 (p 1898-1929).
- *Simultaneous untangling and smoothing of moving grids*; López, E.; Nigro, N. and Storti, M.; Int. J. for Numerical Methods in Engineering 2008, Volume 76 (p 994-1019).
- *Validation of 0D/1D computational code for the design of several kind of internal combustion engines*; López, E. and Nigro, N.; Latin American Applied Research. (submitted)
- *In search of improvements for the computational simulation of internal combustion engines*; López, E.; Toth, J.; Nigro, N. and Storti, M.; chapter book. Nova Science Publishers, Inc.; Frank Columbus Ed. (submitted)

Future work

A great amount of work remains to be done:

- The effective coupling of the 1D/0D code and the CFD-3D code.
- To incorporate the modeling of the spray dynamics, the mixture formation and the combustion process.
- To implement more accurate boundary conditions.
- ...

Gracias por su Atencion